BIOCELL
2024 48(3): 453-462

Tech Science Press

SENEX-mediated CDK4/6 inhibition promotes senescence and confers apoptosis resistance in B-cell non-Hodgkin lymphoma

Jiyu WANG[1,#]; Liuying YI[2,#]; Keke HUANG[1]; Yangyang WANG[1]; Huiping WANG[1]; Zhimin ZHAI[1,*]

[1] Department of Hematology, The Second Affiliated Hospital of Anhui Medical University, Hefei, 230601, China
[2] Department of Hematology, The Fourth Affiliated Hospital, Zhejiang University School of Medicine, Yiwu, 322000, China

Key words: *SENEX*, B-cell non-Hodgkin lymphoma, CDK4/6, G1-S phase transition, Therapy-induced senescence, Apoptosis resistance

Abstract: Background: The primary cause of treatment failure in patients with refractory or relapsed B-cell non-Hodgkin lymphoma (r/r B-NHL) is resistance to current therapies, and therapy-induced senescence (TIS) stands out as a crucial mechanism contributing to tumor drug resistance. Here, we analyzed *SENEX*/Rho GTPase Activating Protein 18 (ARHGAP18) expression and prognostic significance in doxorubicin-induced B-NHL-TIS model and r/r B-NHL patients, investigating its target in B-NHL cell senescence and the effect of combining specific inhibitors on apoptosis resistance in B-NHL-TIS cells. **Methods:** Raji cells were transfected with the human *SENEX* shRNA recombinant lentiviral vector (Sh-*SENEX*) and the empty vector negative (NC) to construct a stable transfection cell line with knockdown of *SENEX*. Effect of *SENEX*-silencing on B-NHL-TIS formation, cell function and cell cycle-related pathways was analyzed. Using doxorubicin (DOX)-inducible senescent B-NHL cells combined with the specific cyclin dependent kinase 4/6 (CDK4/6) inhibitor Palbociclib to observe that blocking CDK4/6 effects on TIS formation. *SENEX* expression of 21 B-NHL patients and 8 healthy controls were analyzed by qRT-PCR, and the correlation between its expression and clinical indicators were evaluated. **Results:** The downregulation of *SENEX* expression promotes G1-S phase transition and apoptosis while inhibiting cell proliferation, collectively suppressing the formation of TIS in B-NHL. Blockade of CDK4/6 promotes the DOX-induced G1 phase arrest to enhance TIS formation in B-NHL cells which can reverse the regulatory effect of silencing *SENEX* on B-NHL cell cycle regulation and senescence. The expression levels of *SENEX* were notably elevated in B-NHL patients compared to healthy controls, and Elevated expression levels of *SENEX* were associated with poor prognosis of B-NHL patients. **Conclusions:** *SENEX* enhances apoptosis resistance in B-NHL by inhibiting CDK4/6, thereby preventing G1-S phase transition and promoting TIS formation.

Abbreviations

B-NHL	B-cell non-Hodgkin lymphoma
TIS	Therapy-induced senescence
ARHGAP18	Rho GTPase Activating Protein 18
DOX	Doxorubicin
DLBCL	Diffuse large B-cell lymphoma
MCL	Mantle cell lymphoma
BL	Burkitt lymphoma
CAR-T	Chimeric Antigen Receptor T-cell
ASCT	Autologous stem cell transplantation
SASP	Senescence-associated secretory phenotypes
GAP	GTPase Activating Protein
PAL	Palbociclib
SA-β-gal	Senescence β-Galactosidase
PI	Propidium iodide
CDK4/6	Cyclin dependent kinase 4/6
CCND1, CCND2, or CCND3	Cyclin D1, D2 or D3
Rb	Retinoblastoma
WBC	White Blood Cell
Hb	Hemoglobin
ALB	Albumin
PLT	Platelet

*Address correspondence to: Zhimin Zhai, zzzm889@163.com
#These authors have contributed equally to this work
Received: 20 November 2023; Accepted: 23 January 2024;
Published: 15 March 2024

Doi: 10.32604/biocell.2024.047871

β2-MG	β2-Microglobulin
LDH	Lactate Dehydrogenase
IPI	International Prognostic Index
p16	Cdkn2a
p21	Cdkn1a

Introduction

Lymphoma comprises a group of malignant tumors originating from the hematopoietic system and is recognized as among the frequently occurring malignancies in China, of which approximately 90% are non-Hodgkin lymphomas, with the majority being B-cell lymphomas (B-NHL), accounting for 70% to 85% of the total [1,2]. The World Health Organization's classification of malignant lymphomas has identified around 50 types of B-cell origin malignant lymphoproliferative diseases, characterized by distinct clinical, pathological, and genetic features. Most of them are generally associated with a favorable prognosis, boasting a 5-year survival rate of approximately 70% [3–5]. B-NHL can manifest in either an aggressive or non-aggressive form. Patients with aggressive or recurrent B-NHL have a poor 5-year survival rate, including common types such as diffuse large B-cell lymphoma (DLBCL), mantle cell lymphoma (MCL), Burkitt lymphoma (BL), and others [6]. Currently, the most prevalent treatment regimen in clinical practice involves immune therapy or new molecular targeted drugs combined with chemotherapy. As an example, the standard treatment for DLBCL involves the combination of rituximab with cyclophosphamide, doxorubicin, vincristine, and prednisone (R-CHOP) regimen, resulting in a cure rate ranging from 50% to 70%. Nevertheless, a considerable number of patients fail to respond to this treatment either owing to a lack of the complementary immune response or resistance to apoptosis, leading to a highly unfavorable prognosis for relapsed or refractory individuals [7,8]. Despite undergoing second-line treatments, including salvage chemotherapy, autologous stem cell transplantation (ASCT), or Chimeric Antigen Receptor T-cell (CAR-T) therapy, around 30%–40% of patients still experience recurrence with a poor prognosis [9,10].

Cellular senescence is a state of stress-responsive cell-cycle arrest and is known to play a vital role in tumor suppression [11,12]. While therapy-induced senescence (TIS) can alter the peripheral immune microenvironment by enhancing senescence-associated secretory phenotypes (SASP), thereby promoting tumor recurrence, metastasis, and resistance to therapy [13–16]. *SENEX* is an innovative gene implicated in cellular senescence, encoding the protein Rho GTPase Activating Protein 18 (ARHGAP18) belonging to the GTPase Activating Protein (GAP) family [17,18]. Our previous studies have found that TIS regulated by *SENEX* induces the accumulation of immunosuppressive cells in the peripheral environment and enhances the SASP [19–21]. However, the impact of *SENEX*-activated TIS on the function of B-NHL cells and the specific underlying mechanisms remains inconclusive. Accordingly, herein, we comprehensively analyzed the expression levels and prognostic significance of *SENEX*/ARHGAP18 in the doxorubicin-induced B-NHL-TIS model as well as in relapsed/refractory B-NHL patients. Moreover, we investigated the target of *SENEX* in regulating B-NHL cell senescence and the effect of combining specific inhibitors of this target on apoptosis resistance of B-NHL-TIS cells. We aim to contribute potential novel TIS markers and therapeutic targets for patients with r/r B-NHL.

Materials and Methods

Patients

From August 2019 to September 2021, 21 individuals diagnosed with B-cell non-Hodgkin lymphoma (B-NHL) and 6 healthy volunteers were included in the study at the Second Hospital of Anhui Medical University. Among them, 15 patients had diffuse large B-cell lymphoma, 1 had mantle cell lymphoma, 2 had follicular lymphoma, 1 had Burkitt lymphoma, and 2 had an undetermined pathological type. Diagnosis and treatment of B-NHL patients followed the criteria of the fourth edition of the World Health Organization lymphoma classification in 2008 and the Chinese guidelines for the diagnosis and treatment of malignant lymphoma (2015 edition). Table 1 presents the detailed clinical data of the patients. The Institutional Review Board (IRB) of the Second Hospital of Anhui Medical University approved this study (LLSC20190034). Informed consent was obtained from all participants, including patients and healthy volunteers.

Cell culture

The human B-NHL cell line Raji was procured from the Shanghai Cell Bank of the Chinese Academy of Sciences (Shanghai, China) and cultured in Roswell Park Memorial Institute-1640 (RPMI-1640, Hyclone, Logan, UT, USA, SH30809.01) medium supplemented with 10%–20% Fetal Bovine Serum (FBS, Lonsera, Uruguay, S711-001S). Cell cultures were maintained at 37°C in a humidified atmosphere with 5% CO_2.

Construction and transduction of shRNA-expressing lentiviral vector

The recombinant lentivirus named *SENEX*i was used to interfere with the *SENEX* expression (Sh-*SENEX*), and an empty carrier lentivirus was used as a negative control (NC). The lentivirus were obtained from GenePharma

TABLE 1

Characteristics of B-NHL patients and healthy controls

Groups	No. of patients	Median age (range)	Gender (M/F)
B-NHL	21	62.33 (29–81)	12/9
ND	9	66.22 (44–80)	5/4
r/r	12	59.41 (29–81)	7/5
Healthy controls	8	53.88 (40–67)	3/5

(Shanghai, China). Raji cells were incubated with the lentivirus for 48 h following the manufacturer's instructions. To establish stable transduced cell clones, the transgenic cells were cultured in a medium supplemented with puromycin. *SENEX* expression levels were quantified using western blot and quantitative reverse transcription-polymerase chain reaction (qRT-PCR).

Drug preparation and treatment

Cyclin dependent kinase 4/6 (CDK4/6) inhibitors (Palbociclib, PAL), acquired from Selleckchem (Houston, Texas, USA, S1116), were dissolved in dimethyl sulfoxide (DMSO, Sangon Biotech, Shanghai, China, ST038) to achieve a concentration of 50 mmol/L. Doxorubicin (DOX, Solarbio, Beijing, China, D8740) was dissolved in double-distilled H_2O to achieve a concentration of 10 mmol/L. Subsequently, the cells were exposed to 40 nM DOX and/or 10 μM PAL for 2 h, followed by replacement with RPMI-1640 medium containing 10% FBS for subsequent analysis.

Senescence β-galactosidase staining

Senescent cells were stained using the Senescence β-Galactosidase Staining Kit (SA-β-gal, Beyotime, Shanghai, China, C0602). Cells were fixed in β-galactosidase staining fixative for 15 min and then incubated with the staining working solution overnight at 37°C without CO_2. Stained cells were observed under a microscope (Olympus Corporation, Japan, IX2-ILL100). Cells exhibiting a green-blue stain were considered positive for senescence.

Senescence β-galactosidase activity assay

The quantitative measurement of SA-β-Gal activity in cells was performed using flow cytometry with the Senescence β-Galactosidase Activity Assay Kit (Cell Signaling Technology, USA, #35302). Cells ($1–2 \times 10^6$ cells/mL) were incubated in medium containing Bafilomycin A1 at 37°C for 1 h. SA-β-Gal substrate solution was then added to cells in a culture medium containing Bafilomycin A1 to produce a 1:200 dilution (33 μM) and incubated at 37°C for 2–4 h. After being washed three times with 1X PBS, the cells were analyzed by flow cytometry (FC500 MPL, Beckman Coulter, Indiana, USA), and senescent cells were identified based on average fluorescence intensity.

Cell viability assay

To assess cell viability, cells subjected to the indicated conditions in a 96-well plate were evaluated using the Cell Counting Kit-8 (CCK-8, Beyotime, Shanghai, China, C0037) following the manufacturer's instructions. 10 μL working solution was added to each well and incubated for 4 h. The optical density values were then measured at 450 nm.

Apoptosis assay

Apoptosis was evaluated utilizing the Annexin V-APC/propidium iodide (PI) apoptosis detection kit (Bestbio, Shanghai, China, BB-41025) following the manufacturer's protocols. Subsequently, cells were suspended in binding buffer and stained with Annexin V-APC and PI. Analysis of apoptotic cells was carried out using a flow cytometer (Cytoflex, Beckman Coulter, Indiana, USA) within 1 h of staining. Data quantification was performed with CytExpert Software (Beckman Coulter, Indiana, USA).

Cell-cycle assay

Cell cycle distribution was assessed using the COULTER DNA PREP Reagents kit (Beckman Coulter, Indiana, USA, 6607055). The staining protocol followed a previously published reference [21], and flow cytometry (FC500 MPL, Beckman Coulter) was employed for data analysis. Kaluza Software (Beckman Coulter, Indiana, USA) was utilized to generate cell cycle phase distributions.

Quantitative Real-Time PCR (qRT-PCR)

Total RNA extraction utilized TRIZOL reagent (Sangon, Shanghai, China, B511311). Subsequently, cDNA synthesis was conducted employing the Revert Aid first-strand cDNA synthesis kit (Thermo Fisher, USA, K1621). qRT-PCR analysis was performed using TB Green® Premix Ex Taq™ II (Tli RNaseH Plus) (Takara, RR420A) on a Bio-Rad CFX96 Connect Real-Time system (Bio-Rad, USA). Primers were provided by Sangon (Shanghai, China). Relative gene expression levels were determined using the $2^{-\Delta\Delta Ct}$ method. Sequences for qRT-PCR primers are detailed in Table 2.

Western blot analysis

Total proteins were extracted employing IP cell lysis buffer (Beyotime, Shanghai, China, P0013B) through standard procedures. Subsequently, these proteins were separated by sodium dodecyl sulfate/polyacrylamide gel electrophoresis (SDS/PAGE) and transferred to polyvinylidene difluoride membranes (Millipore, USA) using the wet transfer method. The membranes were then blocked in 5% skim milk powder dissolved in Tris-buffered Saline solution/0.1% Tween20 (TBST) and incubated overnight at 4°C with the primary antibody. The following day, membranes underwent incubation with the corresponding secondary antibody for 1

TABLE 2

Primer sequences employed for qRT-PCR analysis

Names	Sequences
GAPDH-homo-forward	AGCAAGAGCACAAGAGGAAG
GAPDH-homo-reverse	GGTTGAGCACAGGGTACTTT
SENEX-homo-forward	CGATGATGCCACATTACCTAGT
SENEX-homo-reverse	GGGCTAAATGGCAAACTTTCTT
CDK4-homo-forward	GTGTATGGGGCCGTAGGAAC
CDK4-homo-reverse	CCATAGGCACCGACACCAAT
CDK6-homo-forward	GGTGGCCCTCGGAATAGATG
CDK6-homo-reverse	GCCTGTTCCCACTACTCCAC
CCND1-homo-forward	TGAGGGACGCTTTGTCTGTC
CCND1-homo-reverse	GCCTTTGGCCTCTCGATACA
CCND2-homo-forward	GAAGCTGTCTCTGATCCGCA
CCND2-homo-reverse	TGCTCCCACACTTCCAGTTG
CCND3-homo-forward	ACAGGCCTTGGTCAAAAAGC
CCND3-homo-reverse	ATCATGGATGGCGGGTACAT

TABLE 3

Antibodies used for western blot

Name	Company	Item number	Dilution ratio
Anti-ARHGAP18 antibody	Abcam (Cambridge, UK)	ab262926	1:1000
P16 INK4A(D7C1M) rabbit mAb	Cell Signaling Technology	#80772	1:1000
P21 Waf1/Cip1(12D1) rabbit mAb	Cell Signaling Technology	#2947	1:1000
Rb(D20) rabbit mAb	Cell Signaling Technology	#9313	1:1000
Phospho-Rb rabbit mAb	Cell Signaling Technology	#8180	1:1000
CDK4 (D9G3E) rabbit mAb	Cell Signaling Technology	#12790	1:1000
CDK6 (D4S8S) rabbit mAb	Cell Signaling Technology	#13331	1:1000
B-Actin (13E5) rabbit mAb	Cell Signaling Technology	#4970	1:1000
Goat anti-rabbit IgG	ZSGB-BIO (Beijing, China)	ZB-2301	1:500

h at room temperature. Finally, protein bands were visualized using the SuperSignal™ West Femto Trial Kit (Thermo Fisher, USA, 34094). Details of the primary and secondary antibodies utilized for western blot are presented in Table 3.

Statistical analysis

Statistical analyses were conducted using SPSS 19.0 software (IBM, Chicago, IL, USA) and GraphPad Prism 8.0.2 (GraphPad Software Inc., La Jolla, CA, USA). The *t*-test was employed for comparing quantitative data with a normal distribution, while the One-way ANOVA test was utilized for multiple independent samples. Non-parametric Mann-Whitney test was applied for comparing quantitative data with non-normal distribution between two independent samples. The Kruskal & Wallis Test (non-parametric ANOVA) was used for comparing multiple samples. The correlation between the expression of *SENEX* gene in the peripheral blood of B-NHL patients and clinical data was analyzed using R-studio software. $p < 0.05$ was used to determine statistical significance.

Results

Downregulation of SENEX expression promotes G1-S phase transition and inhibits TIS formation in B-NHL cells

Raji cells were transfected with the human *SENEX* shRNA recombinant lentiviral vector (Sh-*SENEX*) and the empty vector negative (NC) to construct a stable transfection cell

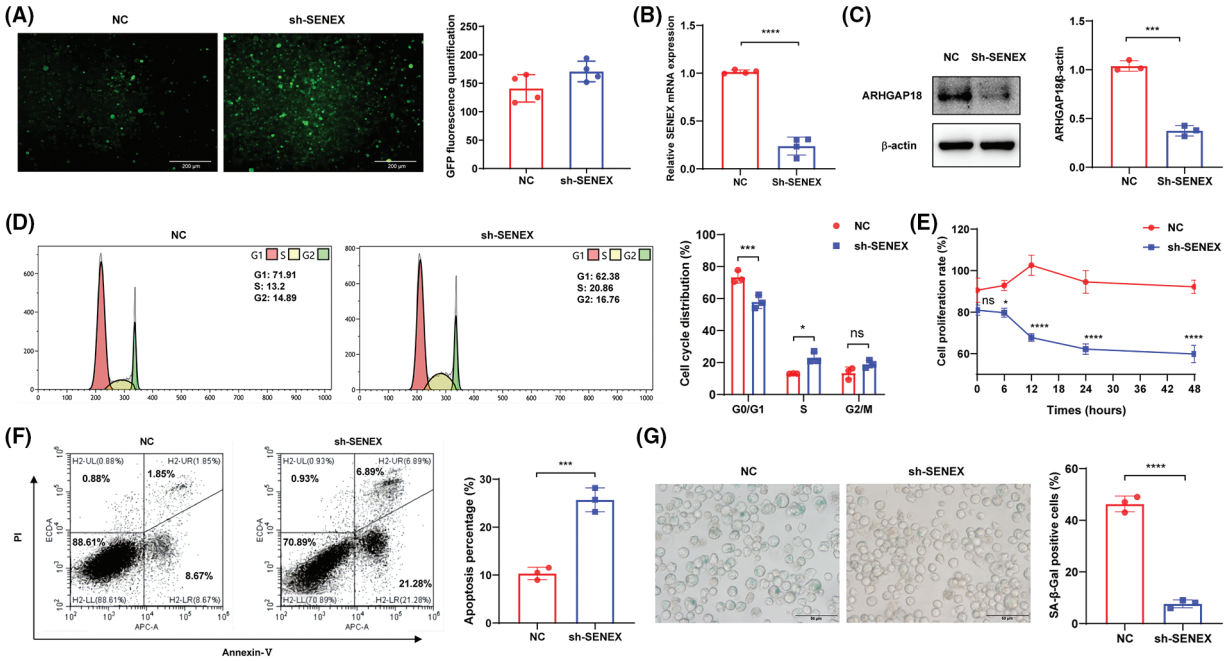

FIGURE 1. Downregulation of *SENEX* expression promotes G1-S phase transition and inhibits TIS formation. (A) Fluorescence analysis in Raji cells transfected with NC/Sh-*SENEX*. (B) Expression of *SENEX* in Raji cells transfected with NC/Sh-*SENEX* by qRT-PCR. (C) Expression of ARHGAP18 in Raji cells transfected with NC/Sh-*SENEX* by western-blot. (D) Cell cycle distribution in Raji cells transfected with NC/Sh-*SENEX* by flow cytometry. (E) Cells viability in Raji cells transfected with NC/Sh-*SENEX* by CCK8 analysis. (F) Apoptosis in Raji cells transfected with NC/Sh-*SENEX* by flow cytometry. (G) Senescence induction by DOX treatment in Raji cells transfected with NC/Sh-*SENEX*, as determined by SA-β-gal staining. Mean percentage ± SD, n = 3 independent experiments, $^{****}p < 0.0001$, $^{***}p < 0.001$ and $^{*}p < 0.05$.

line with knockdown of *SENEX*. Green GFP fluorescence was observed under the fluorescence microscope indicating successful transfection (Fig. 1A). *SENEX* mRNA expression levels and its encoded ARHGAP18 protein were notably reduced in the Sh-*SENEX* group when compared to the NC group (Figs. 1B and 1C). Furthermore, this study examined the differences in cell cycle distribution between the two groups. The results indicated a significant decrease in G0/G1 phase distribution (NC 73.46% *vs.* sh-*SENEX* 57.96%, p = 0.0009) and an increase in S phase cell cycle distribution in the Sh-*SENEX* group (NC 13.07% *vs.* sh-*SENEX* 22.98%, p = 0.0275) (Fig. 1D), suggesting that the downregulation of *SENEX* expression promotes the G1-S phase transition. Cell proliferation capacity was assessed at 0, 6, 12, 24, and 48 h post stable transfection. The results indicated a significant inhibition of cell proliferation in the Sh-*SENEX* group starting from 6 h onwards (Fig. 1E). In contrast, while cell proliferation capacity was significantly inhibited, the proportion of cell apoptosis showed an increasing trend simultaneously (Fig. 1F). Downregulation of *SENEX* expression promoted apoptosis and inhibited proliferation of B-NHL cells. Cells were then treated with DOX, the SA-β-gal staining showed that the proportion of SA-β-gal positive senescent cells in Sh-*SENEX* group were significantly lower than NC group (Fig. 1G), suggesting that downregulation of *SENEX* expression inhibits TIS formation.

Blockade of CDK4/6 promotes the DOX-induced G1 phase arrest to enhance TIS formation in B-NHL cells

Cellular senescence representss a stress-responsive cell-cycle arrest program. CDK4/6 and the complexes formed with cyclin D1, cyclin D2 or cyclin D3 (CCND1, CCND2, or CCND3) are recognized as kinases that regulate the cell cycle, facilitating the G1-S phase transition by promoting the phosphorylation of the retinoblastoma protein (pRb) and subsequently enabling the release of the transcription factor E2F. Herein, the CDK4/6 inhibitor PAL was applied to the DOX-induced TIS model to elucidate the effects on functionality resulting from the blockade of CDK4/6. As compared to control and DOX groups, cell cycle distribution in G1 phase was significantly increased in DOX+PAL group (control 39.63% *vs.* DOX 45.54% *vs.* DOX+PAL 65.12%), suggesting that blockade of CDK4/6 promotes the DOX-induced G1 phase arrest in B-NHL cells (Fig. 2A). To

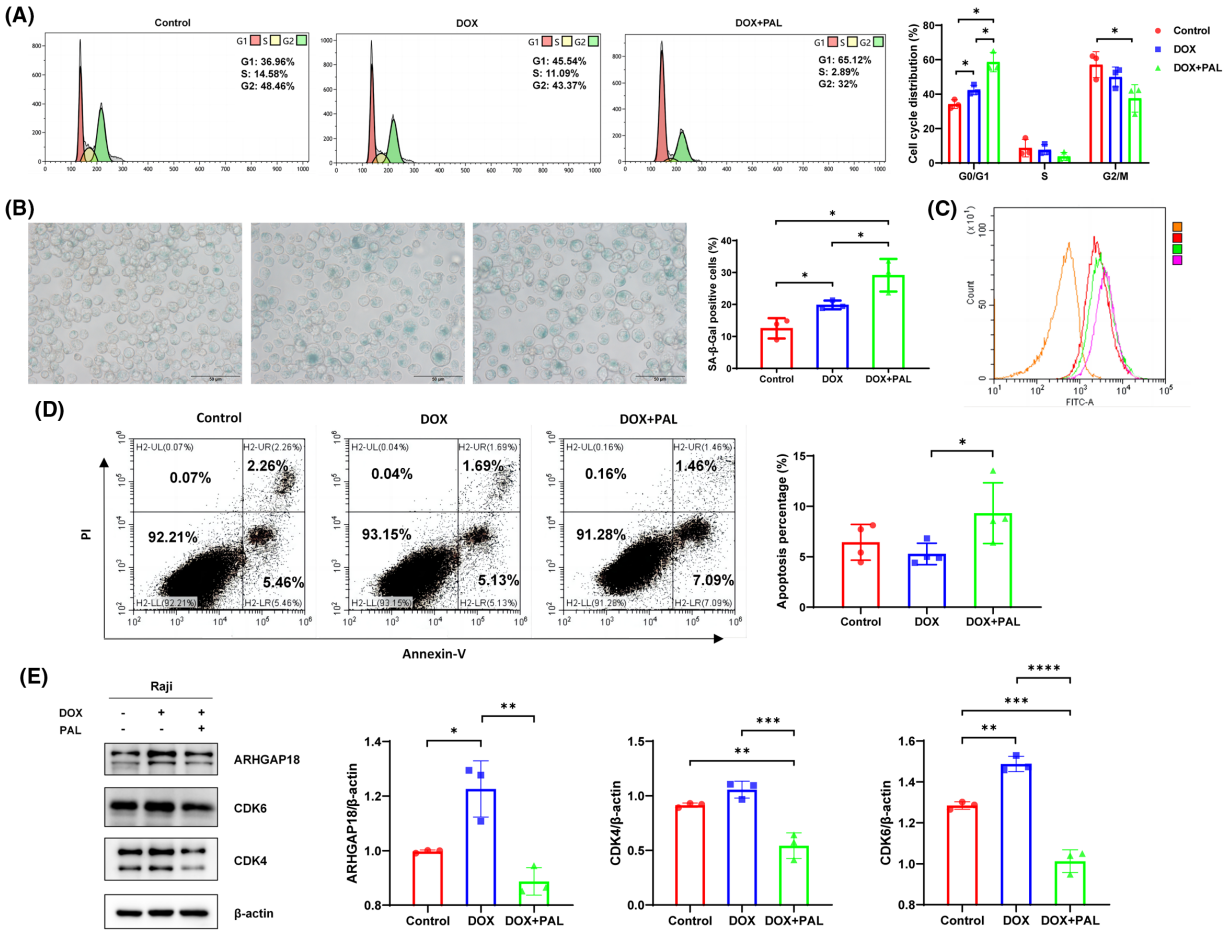

FIGURE 2. Blockade of CDK4/6 promotes the DOX-induced G1 phase arrest to enhance TIS formation in B-NHL cells. (A) Cell cycle distribution in Raji cells treated with DOX/PAL, as determined by flow cytometry. (B) The proportion of SA-β-Gal-positive senescent cells in Raji cells treated with DOX/PAL, as determined by SA-β-gal staining. (C) Mean fluorescence intensity of SA-β-Gal positive cells treated with DOX/PAL by flow cytometry. Orange represents the negative control without antibody, red represents the control group, green represents the DOX group, and purple represents the DOX+PAL group. (D) Apoptosis in Raji cells treated with DOX/PAL, as determined by flow cytometry. (E) The expression levels of CDK4/CDK6 and ARHGAP18 in Raji cells treated with DOX/PAL. Mean percentage ± SD, n = 3 independent experiments, ****p < 0.0001, ***p < 0.001, **p < 0.01 and *p < 0.05.

investigate whether CDK4/6 was involved in *SENEX* regulated TIS formation, PAL was used to treat the DOX-induced B-NHL-TIS model. The results demonstrated a significant increase in the proportion of SA-β-gal-positive senescent cells in the PAL combined with DOX group. Flow cytometry results also indicated an enhancement in the mean fluorescence intensity of SA-β-gal (Figs. 2B and 2C). The apoptosis experiment findings revealed a significant enhancement in the apoptosis rate of Raji cells when PAL was combined with DOX (Fig. 2D). To investigate the interaction between *SENEX* and CDK4/6 in the formation of DOX-induced B-NHL-TIS, we analyzed the expression levels of ARHGAP18 and CDK4/6 in Raji cells treated with a combination of PAL and DOX. In comparison to the control group, the expression levels of CDK4, CDK6, and ARHGAP18 increased in the DOX group. Conversely, in the DOX+PAL group, the expression levels of ARHGAP18 and CDK4/6 were down-regulated compared to the DOX group (Fig. 2E).

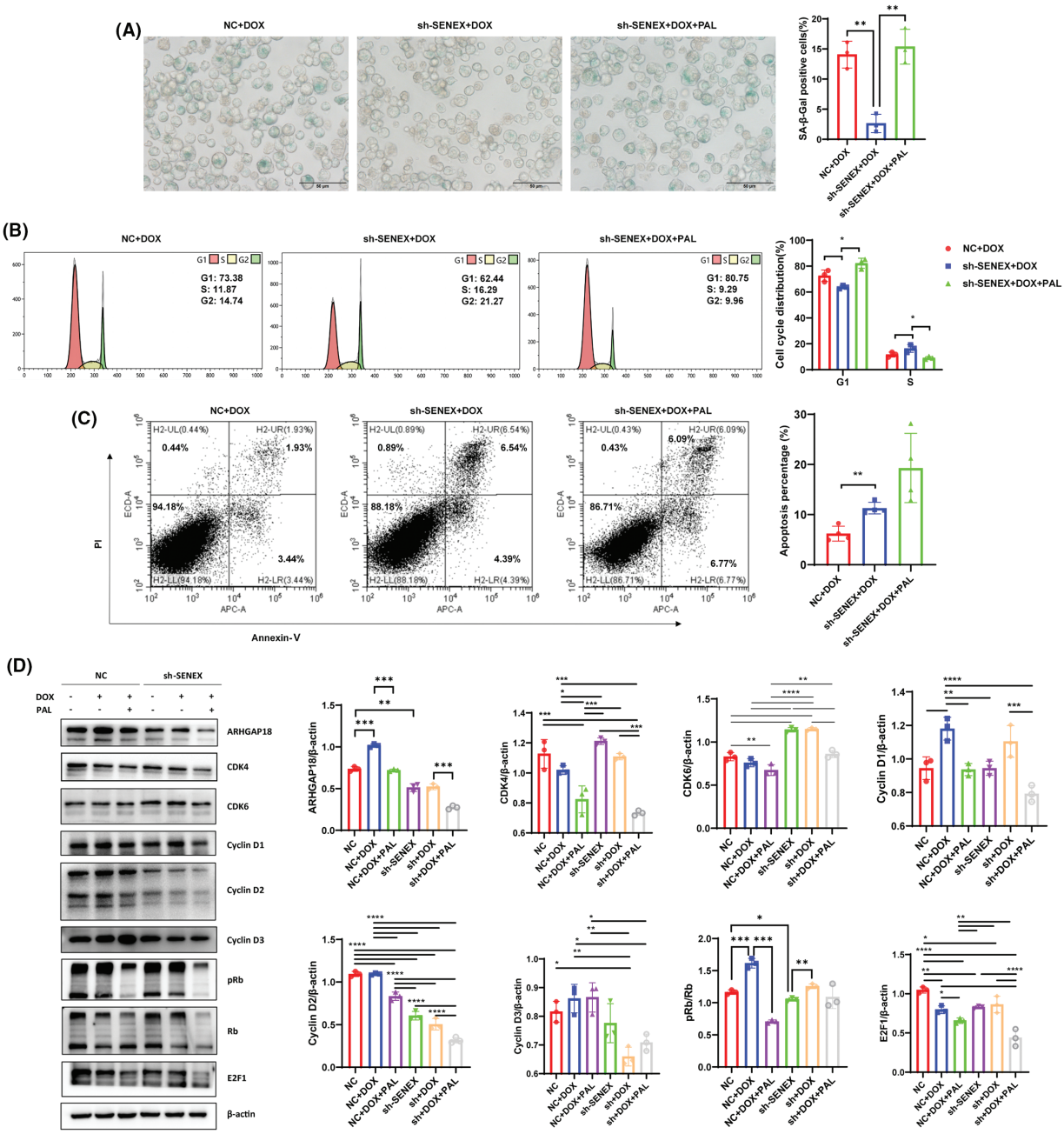

FIGURE 3. Blocking CDK4/6 reverses the regulatory effect of silencing *SENEX* on B-NHL-TIS. (A) The proportion of SA-β-Gal-positive senescent cells in Raji cells treated with DOX/PAL, as determined by SA-β-gal staining. (B) Cell cycle distribution in NC/Sh-*SENEX* transfection cells treated with DOX/PAL, as determined by flow cytometry. From left to right are the NC+DOX group, Sh-*SENEX*+DOX group, and Sh-*SENEX*+DOX+PAL group. (C) Apoptosis in in NC/Sh-*SENEX* transfection cells treated with DOX/PAL, as determined by flow cytometry. (D) The expression of CDK4/CDK6 related pathway and ARHGAP18 in DOX-induced NC and Sh-*SENEX* groups. Mean percentage ± SD, n = 3 independent experiments, $^{****}p < 0.0001$, $^{***}p < 0.001$, $^{**}p < 0.01$ and $^{*}p < 0.05$.

Blockade of CDK4/6 reverses the regulatory effect of silencing SENEX on B-NHL-TIS

Under the same DOX treatment conditions, the proportion of senescent cells in the downregulated *SENEX* expression group decreased significantly. After adding the CDK4/6 inhibitor PAL to the B-NHL cells down-regulating the expression of *SENEX*, the proportion of senescent cells was significantly increased, indicating that blocking CDK4/6 can reverse the regulatory effect of silencing *SENEX* on B-NHL cell senescence (Fig. 3A). Similarly treated with DOX, the downregulated SENEX expression group exhibited a notable decrease in the distribution of cells in the G1 phase, accompanied by a significant increase in the proportion of cells in the S phase. However, upon the concurrent application of the CDK4/6 inhibitor PAL, the Sh-SENEX group demonstrated an increase in the proportion of cells in the G1 phase and a decrease in the proportion of cells in the S phase. This suggests that blocking CDK4/6 has the potential to reverse the impact of down-regulating SENEX expression on B-NHL cell cycle regulation (Fig. 3B). Also exposed to DOX, the percentage of apoptosis in the Sh-*SENEX* group was higher than that in the control group, indicating that down-regulating the expression of *SENEX* can reduce the apoptosis resistance of B-NHL cells to the chemotherapeutic drug DOX. The proportion of apoptotic cells tended to increase after the treatment of DOX and PAL in the cells down-regulating the expression of *SENEX*, and PAL combined with the chemotherapy drug DOX could increase the killing effect on B-NHL cells (Fig. 3C). To delineate the molecular mechanisms underlying the association of ARHGAP18 silencing with CDK4/6 suppression in B-NHL-TIS, we profiled expression levels of cell cycle related pathways in DOX-induced B-NHL-TIS. Because ARHGAP18 interacts with CDK4/6 to aid TIS, we hypothesize that, in the absence of ARHGAP18, B-NHL can no longer trigger TIS formation, by acting on CDK4/6-associated pathways. ARHGAP18 is significantly activated in DOX-induced B-NHL-TIS cells, and inhibition of ARHGAP18 results in increased expression of CDK4/6 and pRb, as well as decreased levels of free E2F1 and Cyclin D2. Blocking CDK4/6 can reverse the increase in Rb phosphorylation induced by ARHGAP18 inhibition (Fig. 3D). Although we cannot completely exclude alternative explanations, these and the subsequent data strongly favor ARHGAP18/*SENEX* can regulate cell senescence and promote apoptosis resistance of B-NHL cells by inhibiting CDK4/6 pathway as the most compelling and consistent interpretation of the observations presented.

Expression analysis and clinical relevance of SENEX/CDK4/CDK6 in patients with B-NHL

In this analysis, 21 patients diagnosed with B-NHL and 8 healthy controls were included. The average age of newly diagnosed B-NHL patients was 62.33 (29–81) years old, and 12 (57%) were male, 9 (43%) were female. The average age of healthy controls was 53.88 (40–67) years old, and 3 (37.5%) were male, 5 (62.5%) were female. Table 1 presents the clinical characteristics of the patients included in this study. No significant differences in gender and age were observed between the two groups. To explore the expression levels of *SENEX*/CDK4/CDK6 in peripheral blood of patients with B-NHL, this study analyzed the expression

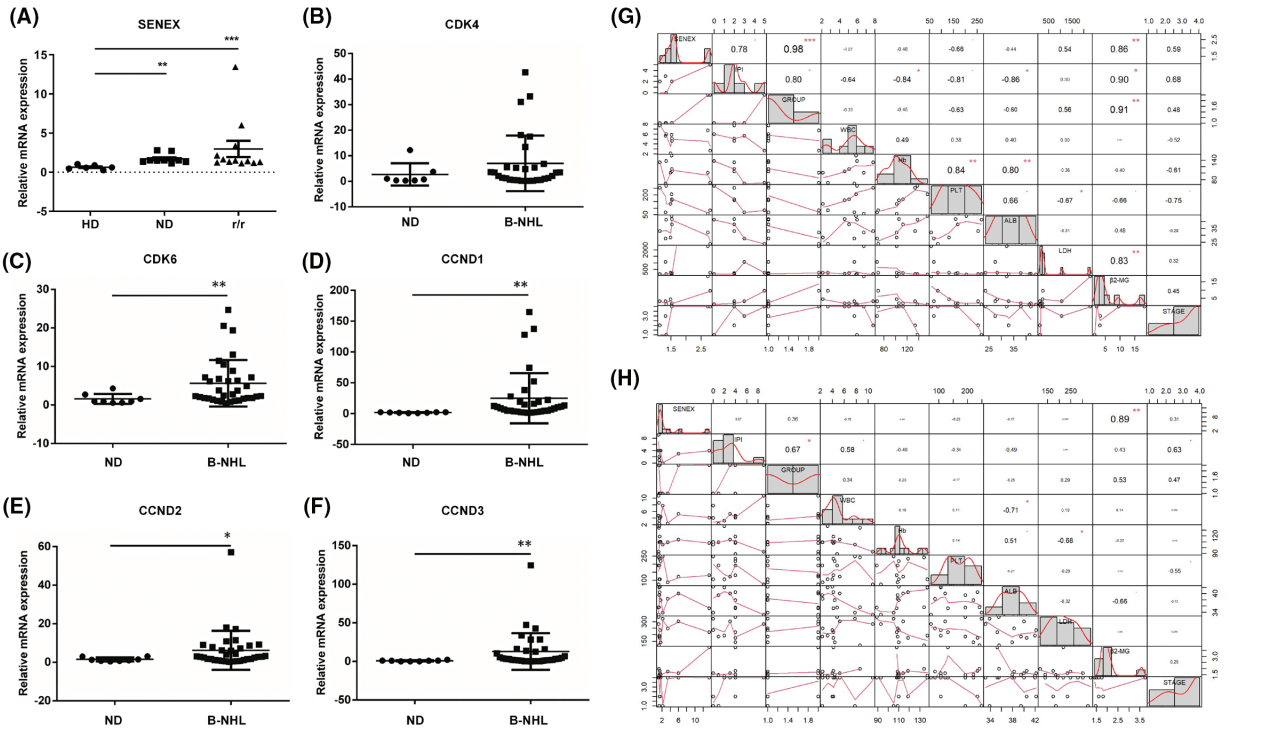

FIGURE 4. Expression analysis and clinical relevance of *SENEX*/CDK4/CDK6 in patients with B-NHL. (A–F) The expression of *SENEX* and CDK4/6-CCND signaling axis in B-NHL patients. (A) *SENEX*, (B) CDK4, (C) CDK6, (D) CCND1, (E) CCND2, and (F) CCND3. (G) The correlation between the expression level of *SENEX* and clinical data in newly diagnosed B-NHL patients. (H) The correlation between the expression level of *SENEX* and clinical data in r/r B-NHL patients. ***$p < 0.001$, **$p < 0.01$ and *$p < 0.05$.

levels of *SENEX*/CDK4/CDK6 in peripheral blood of 21 B-NHL patients (including 9 newly diagnosed (ND group) and 12 relapsed or refractory (r/r group) B-NHL patients) and 8 or 6 healthy controls. Compared with healthy adults, the expression levels of *SENEX* in peripheral blood of both ND and r/r groups of B-NHL patients were significantly elevated (Fig. 4A). Moreover, there was a trend of increased expression of *SENEX* gene in r/r group of B-NHL patients compared to ND group of B-NHL patients (Fig. 4A). Compared to healthy controls, the expression of CDK6 and CCND1/2/3 were significantly increased in the patients with B-NHL (Figs. 4B–4F). Moreover, data were collected on White Blood Cell (WBC), Hemoglobin (Hb), Platelet (PLT), Albumin (ALB), Lactate Dehydrogenase (LDH), β2-Microglobulin (β2-MG), disease stage, grouping, and International Prognostic Index (IPI) score of patients at admission, and performed correlation analysis between these variables and the expression levels of *SENEX* gene using R programming language. The results showed that in the ND group of patients, the expression level of *SENEX* gene was positively correlated with IPI score, disease grouping, LDH, β2-MG, and disease stage. Among these, the expression level of *SENEX* gene was significantly positively correlated with IPI score ($r = 0.78$, $p < 0.05$), disease grouping ($r = 0.98$, $p < 0.001$), and β2-MG level ($r = 0.86$, $p < 0.01$) (Fig. 4G). In the R/R group of B-NHL patients, the expression level of *SENEX* gene was significantly positively correlated with β2-MG level ($r = 0.89$, $p < 0.01$) (Fig. 4H).

Discussion

Over the past two decades, there have been exciting advancements in the diagnosis and treatment of B-NHL. However, a subset of patients with aggressive or relapsed forms of B-NHL develops resistance to existing therapeutic approaches, leading to treatment failure and, ultimately, mortality due to disease progression. Hence, it is crucial to investigate an alternative molecular approach to enhance comprehension of r/r B-NHL and discover potential novel therapeutic targets. The "double-edged sword effect" of TIS and its crucial role in tumor relapse, drug resistance, and treatment resistance are increasingly recognized [22,23]. Senotherapeutics is a novel concept that combines cancer treatment modalities, such as radiation or chemotherapy, inducing senescence in tumor cells, with the induction of apoptosis in senescent cells [24]. However, the current exploration is limited by the high heterogeneity of senescent cells. Senescent cells exhibit elevated expressions of cell cycle regulators, including Cdkn2a (p16) and Cdkn1a (p21), which play a role in regulating cell cycle arrest [25,26]. However, p16/p21 may not function as a specific or sensitive indicator of cellular senescence, as not all cells exhibiting elevated levels of p16 are necessarily in a senescent state, and some senescent cells may lack expression of p16/p21 [25–28]. Studies have initiated the exploration of the notable diversity in cellular senescence across various tissues, underscoring the significance of discovering markers for cellular senescence beyond p16/p21. In this study, we identified a new B-NHL-TIS-specific marker gene, *SENEX*, which is significantly highly expressed in DOX-induced B-NHL senescent cells and is associated with clinical relapse.

ARHGAP18/*SENEX*, also known as Rho GTPase activating protein 18, is a novel endogenous protein participating in diverse physiological and pathological processes, including cellular senescence, cancer, angiogenesis, and immune function. Although research on ARHGAP18/*SENEX* is still in its early stages, studies suggest that its aberrant expression is associated with tumorigenesis and cancer progression. Knockout of ARHGAP18/*SENEX* in mice resulted in the faster formation of subcutaneous melanoma, related to excessive tumor angiogenesis, despite ARHGAP18/*SENEX* having an inhibitory effect on angiogenesis. Furthermore, it serves as a cancer risk locus in breast, lung, and ovarian cancers [29–31]. In this investigation, *SENEX* expression levels were notably elevated in both newly diagnosed and r/r B-NHL patients compared to those in healthy controls. The relapsed/refractory group had a trend of increased *SENEX* expression compared to the newly diagnosed group, but the difference was not statistically significant, which may be related to the small sample size. Furthermore, the expression of *SENEX* in the newly diagnosed B-NHL patients was significantly positively correlated with IPI score and β2-MG level. The expression of *SENEX* in the relapsed/refractory B-NHL patients was significantly positively correlated with β2-MG level. The IPI assessment system includes factors that reflect tumor biology, impact on patients, and responsiveness to treatment. It is an internationally recognized effective and practical prognostic evaluation system. For patients with an IPI score > 2, it often indicates a poor prognosis. β2-MG serves as a β-light chain component of human leukocyte antigen molecules, playing a primary role in lymphocyte surface recognition and its association with killer cell receptors. There have been many studies showings that an elevated level of β2-MG is an independent risk factor for prognosis in B-NHL patients and is related to the survival of lymphoma patients [32–35]. Our results indicate higher expression levels of *SENEX*, CDK6, CCND1, CCND2, and CCND3 compared to normal samples. Furthermore, we observed a correlation between high expression of the *SENEX* gene and poor prognosis in B-NHL patients, suggesting that the *SENEX*/CDK/CCND signaling axis may hold prognostic value for B-NHL.

Further exploration of the interaction between *SENEX* and CDK4/6 in DOX-induced B-NHL-TIS revealed that *SENEX* mediated CDK4/6 inhibition to promoted TIS formation, and conferred apoptosis resistance in B-NHL. Firstly, the downregulation of *SENEX* expression not only promoted apoptosis but also inhibited the proliferation of B-NHL cells. Additionally, it facilitated the G1-S phase transition while concurrently inhibiting TIS formation. Blockade of CDK4/6 promotes the DOX-induced G1 phase arrest to enhance TIS formation in B-NHL cells. Inhibiting CDK4/6 can reverse the regulatory effect of *SENEX* silencing on B-NHL cell senescence and cell cycle in the TIS model. Meanwhile, it was found that under the same DOX treatment conditions, *SENEX* silencing can significantly increase the proportion of apoptotic cells, which again proves the crucial role of CDK4/6 activity inhibition in

inducing TIS and that *SENEX* triggers TIS through this key molecule to protect B-NHL cells. *SENEX* inhibits the G1-S phase transition of B-NHL cells by inhibiting the CDK4/6 pathway, promotes B-NHL cell apoptosis resistance, thereby making lymphoma cells resistant to the killing of chemotherapy drugs and promoting tumor recurrence/ treatment resistance. Results above suggest that ARHGAP18 can induce B-NHL-TIS through suppressing the CDK4/6 pathway, which leads to the arrest of G1-S phase and promotes apoptosis resistance of B-NHL cells. However, it is important to acknowledge some limitations in our study. Firstly, the findings are based on *in vitro* and *ex vivo* experiments, and translating these results to the complex *in vivo* tumor microenvironment may require further validation. Additionally, while our clinical analysis revealed correlations between *SENEX* expression and certain prognostic factors, the relatively small sample size limits the generalizability of these findings.

In summary, this study investigated the impact of downregulating *SENEX* expression on B-NHL-TIS, revealing that *SENEX*-mediated CDK4/6 inhibition promotes senescence and confers apoptosis resistance in B-NHL. Silencing *SENEX* led to a decrease in senescent cells, increased apoptosis, and inhibited proliferation of B-NHL cells. Moreover, blocking CDK4/6 enhanced DOX-induced G1 phase arrest and TIS formation. We further explored the molecular mechanisms, demonstrating that ARHGAP18/ *SENEX* regulates cell senescence and apoptosis resistance by inhibiting the CDK4/6 pathway. Clinical analysis in B-NHL patients confirmed elevated expression of *SENEX*, CDK6, and CCND1/2/3 in peripheral blood, with *SENEX* expression positively correlated with adverse prognostic factors such as IPI score, disease grouping, LDH, and β2-MG levels. These observations provide valuable perspectives on the potential therapeutic targeting of *SENEX* and TIS in r/r B-NHL.

Acknowledgement: None.

Funding Statement: This work was supported by the Major Subject of Science and Technology of Anhui Province (Grant Number: 201903a07020030).

Author Contributions: Study conception and design: Zhimin Zhai and Jiyu Wang; data collection: Keke Huang and Yangyang Wang; analysis and interpretation of results: Liuying Yi and Huiping Wang; draft manuscript preparation: Jiyu Wang. All authors reviewed the results and approved the final version of the manuscript.

Availability of Data and Materials: The datasets used and/or analyzed during the current study are available from the corresponding author on reasonable request.

Ethics Approval: This study was approved by the Institutional Review Board (IRB) Institutional of the Second Hospital of Anhui Medical University (LLSC20190034). Informed consent was obtained from all participants, including patients and healthy volunteers.

Conflicts of Interest: The authors declare that they have no conflicts of interest to report regarding the present study.

References

1. Liu W, Liu J, Song Y, Wang X, Zhou M, Wang L, et al. Mortality of lymphoma and myeloma in China, 2004–2017: an observational study. J Hematol Oncol. 2019;12(1):22.
2. Sung H, Ferlay J, Siegel RL, Laversanne M, Soerjomataram I, Jemal A, et al. Global Cancer Statistics 2020: GLOBOCAN estimates of incidence and mortality worldwide for 36 cancers in 185 countries. CA Cancer J Clin. 2021;71(3):209–49.
3. Polyatskin IL, Artemyeva AS, Krivolapov YA. Revised WHO classification of tumors of hematopoietic and lymphoid tissues, 2017 (4th edition): lymphoid tumors. Arkhiv Patologii. 2019; 81(3):59–65.
4. Grimm KE, O'Malley DP. Aggressive B cell lymphomas in the 2017 revised WHO classification of tumors of hematopoietic and lymphoid tissues. Ann Diagn Pathol. 2019;38:6–10.
5. Alaggio R, Amador C, Anagnostopoulos I, Attygalle AD, Araujo IBO, Berti E, et al. The 5th edition of the World Health Organization classification of haematolymphoid tumours: lymphoid neoplasms. Leukemia. 2022;36(7):1720–48.
6. Alizadeh AA, Eisen MB, Davis RE, Ma C, Lossos IS, Rosenwald A, et al. Distinct types of diffuse large B-cell lymphoma identified by gene expression profiling. Nature. 2000;403(6769):503–11.
7. Susanibar-Adaniya S, Barta SK. Update on diffuse large B cell lymphoma: a review of current data and potential applications on risk stratification and management. Am J Hematol. 2021;96(5):617–29.
8. He MY, Kridel R. Treatment resistance in diffuse large B-cell lymphoma. Leukemia. 2021;35(8):2151–65.
9. Schuster SJ, Svoboda J, Chong EA, Nasta SD, Mato AR, Anak O, et al. Chimeric antigen receptor T cells in refractory B-cell lymphomas. N Engl J Med. 2017;377(26):2545–54.
10. Ernst M, Oeser A, Besiroglu B, Caro-Valenzuela J, Abd El Aziz M, Monsef I, et al. Chimeric antigen receptor (CAR) T-cell therapy for people with relapsed or refractory diffuse large B-cell lymphoma. Cochrane Database Syst Rev. 2021;9(9):CD013365.
11. Munoz-Espin D, Serrano M. Cellular senescence: from physiology to pathology. Nat Rev Mol Cell Biol. 2014;15(7):482–96.
12. Perez-Mancera PA, Young AR, Narita M. Inside and out: the activities of senescence in cancer. Nat Rev Cancer. 2014;14(8):547–58.
13. Victorelli S, Salmonowicz H, Chapman J, Martini H, Vizioli MG, Riley JS, et al. Apoptotic stress causes mtDNA release during senescence and drives the SASP. Nature. 2023;622(7983):627–36.
14. Milanovic M, Fan DNY, Belenki D, Dabritz JHM, Zhao Z, Yu Y, et al. Senescence-associated reprogramming promotes cancer stemness. Nature. 2018;553(7686):96–100.
15. Takasugi M, Yoshida Y, Hara E, Ohtani N. The role of cellular senescence and SASP in tumour microenvironment. FEBS J. 2023;290(5):1348–61.
16. Yang K, Li X, Xie K. Senescence program and its reprogramming in pancreatic premalignancy. Cell Death Dis. 2023;14(8):528.
17. Coleman PR, Hahn CN, Grimshaw M, Lu Y, Li X, Brautigan PJ, et al. Stress-induced premature senescence mediated by a novel gene, *SENEX*, results in an anti-inflammatory phenotype in endothelial cells. Blood. 2010;116(19):4016–24.
18. Lovelace MD, Powter EE, Coleman PR, Zhao Y, Parker A, Chang GH, et al. The RhoGAP protein ARHGAP18/SENEX localizes to microtubules and regulates their stability in endothelial cells. Mol Biol Cell. 2017;28(8):1066–78.
19. Wang J, Tao Q, Pan Y, Wanyan Z, Zhu F, Xu X, et al. Stress-induced premature senescence activated by the *SENEX* gene

mediates apoptosis resistance of diffuse large B-cell lymphoma via promoting immunosuppressive cells and cytokines. Immun Inflamm Dis. 2020;8(4):672–83.

20. Wang J, Wang Z, Wang H, Wanyan Z, Pan Y, Zhu F, et al. Stress-induced premature senescence promotes proliferation by activating the SENEX and p16(INK4a)/Retinoblastoma (Rb) pathway in diffuse large B-cell lymphoma. Turk J Haematol. 2019;36(4):247–54.
21. Wang J, Pan Y, Wan Y, Wanyan Z, Wang Z, Tao Q, et al. SENEX gene promotes cell proliferation by activating RB/E2F pathway in diffuse large B-cell lymphoma cells. BIOCELL. 2021;45(4):933–42.
22. Morales-Valencia J, Lau L, Marti-Nin T, Ozerdem U, David G. Therapy-induced senescence promotes breast cancer cells plasticity by inducing Lipocalin-2 expression. Oncogene. 2022;41(38):4361–70.
23. Prasanna PG, Citrin DE, Hildesheim J, Ahmed MM, Venkatachalam S, Riscuta G, et al. Therapy-induced senescence: opportunities to improve anticancer therapy. J Natl Cancer Inst. 2021;113(10):1285–98.
24. Myrianthopoulos V, Evangelou K, Vasileiou PVS, Cooks T, Vassilakopoulos TP, Pangalis GA, et al. Senescence and senotherapeutics: a new field in cancer therapy. Pharmacol Ther. 2019;193:31–49.
25. Hall BM, Balan V, Gleiberman AS, Strom E, Krasnov P, Virtuoso LP, et al. p16(Ink4a) and senescence-associated beta-galactosidase can be induced in macrophages as part of a reversible response to physiological stimuli. Aging. 2017;9(8):1867–84.
26. Yosef R, Pilpel N, Papismadov N, Gal H, Ovadya Y, Vadai E, et al. p21 maintains senescent cell viability under persistent DNA damage response by restraining JNK and caspase signaling. EMBO J. 2017;36(15):2280–95. doi:10.15252/embj.201695553.
27. Sturmlechner I, Zhang C, Sine CC, van Deursen EJ, Jeganathan KB, Hamada N, et al. p21 produces a bioactive secretome that places stressed cells under immunosurveillance. Sci. 2021; 374(6567):eabb3420. doi:10.1126/science.abb3420.
28. Cohn RL, Gasek NS, Kuchel GA, Xu M. The heterogeneity of cellular senescence: insights at the single-cell level. Trends Cell Biol. 2023;33(1):9–17.
29. Rao N, Lee YF, Ge R. Novel endogenous angiogenesis inhibitors and their therapeutic potential. Acta Pharmacol Sin. 2015; 36(10):1177–90.
30. Chang GH, Lay AJ, Ting KK, Zhao Y, Coleman PR, Powter EE, et al. ARHGAP18: an endogenous inhibitor of angiogenesis, limiting tip formation and stabilizing junctions. Small GTPases. 2014;5(3):1–15.
31. Liang L, Gu W, Li M, Gao R, Zhang X, Guo C, et al. The long noncoding RNA HOTAIRM1 controlled by AML1 enhances glucocorticoid resistance by activating RHOA/ROCK1 pathway through suppressing ARHGAP18. Cell Death Dis. 2021;12(7):702.
32. International Non-Hodgkin's Lymphoma Prognostic Factors Project. A predictive model for aggressive non-Hodgkin's Lymphoma. N Engl J Med. 1993;329(14):987–94.
33. Shipp MA. Prognostic factors in aggressive non-Hodgkin's lymphoma: who has "high-risk" disease? Blood. 1994;83(5): 1165–73.
34. Bai Z, Li L, Guan T, Wang J, Zhao J, Su L. Clinical prognosis and bioinformatic analysis of primary thyroid lymphoma. Med. 2021;100(6):e24598.
35. Lu J, Wu Y, Li B, Luo X, Zhang W, Zeng Y, et al. Predictive value of serological factors, maximal standardized uptake value and ratio of Ki67 in patients diagnosed with non-Hodgkin's lymphoma. Oncol Lett. 2020;20(4):47.